C. D. Hopkins
Department of Mechanical and Aerospace Engineering, The Ohio State University, Columbus, OH 43210
e-mail: hopkins.626@osu.edu

P. J. Wolcott
Department of Mechanical and Aerospace Engineering, The Ohio State University, Columbus, Ohio 43221,
e-mail: wolcott.27@osu.edu

M. J. Dapino[1]
Department of Mechanical and Aerospace Engineering, E307 Scott Laboratory, The Ohio State University, 201 W. 19th Avenue, Columbus, OH 43210
e-mail: dapino.1@osu.edu

A. G. Truog
Welding Engineering Program, Department of Materials Science and Engineering, The Ohio State University, Columbus, OH 43221
e-mail: truog.1@osu.edu

S. S. Babu
Welding Engineering Program, Department of Materials Science and Engineering, The Ohio State University, Columbus, OH 43221
e-mail: babu.13@osu.edu

S. A. Fernandez
Center for Biostatistics, The Ohio State University, Columbus, OH 43210
e-mail: fernandez.71@osu.edu

Optimizing Ultrasonic Additive Manufactured Al 3003 Properties With Statistical Modeling

Ultrasonic additive manufacturing (UAM) has proven useful in the solid-state, low tempe'rature fabrication of layered solid metal structures. It is necessary to optimize the various process variables that affect the quality of bonding between layers through investigation of the mechanical strength of various UAM builds. We investigate the effect of the process parameters tack force, weld force, oscillation amplitude, and weld rate on the ultimate shear strength (USS) and ultimate transverse tensile strength (UTTS) of 3003-H18 aluminum UAM built samples. A multifactorial experiment was designed and an analysis of variance was performed to obtain an optimal set of process parameters for maximizing mechanical strength for the tested factors. The statistical analyses indicate that a relatively high mechanical strength can be achieved with a process window bounded by a 350 N tack force, 1000 N weld force, 26 μm oscillation amplitude, and about 42 mm/s weld rate. Optical analyses of bond characterization did not show a consistent correlation linking linear weld density and bonded area of fractured surfaces to mechanical strength. Therefore, scanning electronmicroscopy (SEM) was conducted on fractured samples showing a good correlation between mechanical strength and area fraction that shows ductile failure. [DOI: 10.1115/1.4005269]

1 Introduction

Ultrasonic additive manufacturing (UAM) is an emerging solid-state joining process that uses layered manufacturing techniques in combination with principles of ultrasonic metal welding and subtractive processes to create near net shape metal parts [1]. In this process, a rolling weld horn applies ultrasonic energy over thin metal tapes to form nascent surfaces and clean metal-to-metal bonding well below the melting temperature of the foil material [2]. The UAM process has a number of input parameters that can be adjusted to optimize the bonding between metal layers [3]. These parameters include tack force, weld force, oscillation amplitude, and weld rate [3]. The optimal parameters for a given application depend on the foil material and machine capabilities. It is therefore necessary to conduct experimental studies to determine the ideal process parameters for a given application.

Commonly, investigations of the input parameters are related to the bond quality of UAM builds. Bond quality has been determined using peel strength data or linear weld density (LWD) [4–7]. However, neither of these characteristics directly correlates to material properties commonly used. This study focuses on relating UAM manufacturing settings to the ultimate shear strength (USS) and ultimate transverse tensile strength (UTTS) of 3003 aluminum builds whose height is much greater than the one or two layer builds often used in peel strength or linear weld density testing. A statistical analysis was conducted to account for the stochastic nature of the UAM process and determine the optimal set of input parameters to maximize mechanical strength. Previous work has been conducted using a similar experimental model for statistical characterization of Ti/Al composites [3]. A generalized linear model was used and main effects, interactions and trends of the UAM manufacturing settings on the USS and UTTS were investigated. The observed properties were correlated

[1]Corresponding author.

Contributed by the Materials Division of ASME for publication in the JOURNAL OF ENGINEERING MATERIALS AND TECHNOLOGY. Manuscript received November 29, 2010; final manuscript received August 24, 2011; published online December 6, 2011. Assoc. Editor: Thomas Siegmund.

Table 1 Process parameters and levels used for Al 3003 DOE

Parameter	Level 1	Level 2	Level 3
Tack force (N)	200	350	—
Weld force (N)	600	800	1000
Oscillation amplitude (μm)	18	22	26
Weld rate[a] (in/min)	100	125	150
—	(42 mm/s)	(53 mm/s)	(64 mm/s)

[a]Default machine input unit is in/min. Values in mm/sec are rounded off to nearest integer.

Table 2 Constants during experiments

Process variable	Set value
Tack rate (in/min)	120
—	(50.8 mm/s)
Tack amplitude (μm)	9
Spot time (s)	0
Base plate temperature (°C)	149
Sonotrode surface texture, Ra (μm)	7
Oscillation frequency (kHz)	20

Table 3 Treatment combinations from pilot experiments that were unsuccessful in creating builds

Pilot experiment	Tack force (N)	Weld force (N)	Amplitude (μm)	Weld rate (mm/s)
1	350	1500	32	53
2	350	1500	30	53
3	350	1500	26	53
4a	350	500	22	42
4b	350	1100	26	53

with LWD and with the percentage of bonded area per fracture surface for high, medium, and low strength samples. Electron microscopy was used to gain further insight into the bonding mechanisms in UAM builds and show a correlation between bond strength and bonded area.

2 Experimental Methods

2.1 Sample Fabrication and Statistical Procedures. The material used in this study is 0.006″ (152.4 μm) thick tapes of 3003 H-18 aluminum built on a 3003 H-14 aluminum base plate. All samples were built at Edison Welding Institute, Columbus, OH, using a Solidica, Inc., Formation machine. Sequential joining of tape layers was achieved through tacking and welding passes where the magnitude of the process parameters in the weld pass is generally higher than the tack pass [8].

A Taguchi L18 orthogonal array was employed for the experimental design. The Taguchi array is a statistically robust design that reduces the number of treatment combinations from 54 to 18 for a design consisting of three parameters at three levels each and one parameter at two levels [9]. The process parameters and their corresponding levels were selected from pilot tests determining viable builds as shown in Table 1. The levels of the manufacturing parameters were selected to create an even distribution across the range of operation limits (not machine capabilities) based upon pilot experiments. Table 2 summarizes all other conditions that were held constant during the experiments.

The unsuccessful treatment combinations from the pilot experiments are shown in Table 3. The data shows that there is an upper and lower threshold to combinations of weld force and oscillation amplitude. If the amplitude and weld force are too high, the tape layer welds to the sonotrode. In contrast, if the weld force and oscillation amplitude are too low, no bonding occurs.

Table 4 Coded Taguchi L18 orthogonal array

Experiment number	Treatment combination	Tack force	Weld force	Amplitude	Weld rate
3	1	1	1	1	1
11	2	1	1	2	2
8	3	1	1	3	3
14	4	1	2	1	1
15	5	1	2	2	2
10	6	1	2	3	3
13	7	1	3	1	2
9	8	1	3	2	3
6	9	1	3	3	1
17	10	2	1	1	3
1	11	2	1	2	1
16	12	2	1	3	2
12	13	2	2	1	2
5	14	2	2	2	3
7	15	2	2	3	1
18	16	2	3	1	3
4	17	2	3	2	1
2	18	2	3	3	2

Table 4 shows the Taguchi orthogonal array with coded parameter levels. The treatment combinations were randomized and were built and tested according to the randomized order (Experiment Number) to avoid any bias due to build order. The statistical model used for this design of experiment (DOE) was a generalized linear model with four main effects. The linear model equation is

$$Y_{ijklt} = \mu + \alpha_i + \beta_j + \gamma_k + \delta_l + \epsilon_{ijklt} \quad (1)$$

where it is assumed that ϵ_{ijklt} is of a normal distribution about zero and all ϵ_{ijklt} are mutually independent with $i = 1,2$; $j = k = l = 1, 2, 3$; $t = 1, 2, 3, 4$.

Equation (1) summarizes the dependence of the response variable (USS or UTTS), Y_{ijklt}, upon the levels of the treatment factors [10]. Parameter μ denotes the overall mean of the response variable. The effects of each of the process parameters on the mean response are represented by α_i, β_j, γ_k, and δ_l, where α_i is the effect of tack force at the ith level on the response while the other three factors are fixed. Similarly, β_j, γ_k, and δ_l represent the effects of weld force, amplitude, and weld rate at the jth, kth, and lth levels, respectively, while the other factors are fixed. The error variable, ϵ_{ijklt} is a random variable with zero mean and denotes any nuisance variation in the response. After testing the main effects, two-way interactions were included in the model, one at a time to determine their significance.

Four shear and four transverse tensile samples were intended for testing per treatment combination. All mechanical tests were run on a 20 kip (89 kN) Interlaken load frame fitted with a ± 5000 lb (22.2 kN) load cell placed in series with the load train. The load frame was connected to an MTS 458.20 Micro Console controller coupled to a data acquisition system comprising a Data Physics Mobilyzer and PC. All tests were run under displacement control with a ramp (average rate of 0.254 mm/s) and hold input program. During testing, displacement was measured using the linear variable differential transformer (LVDT) integrated into the load frame. Since the LVDT measures deflection of the load frame actuator, all displacement data include displacement within the load train and the specimen. Due to this, the resulting force– displacement plots can only be used to determine if a given sample failed in brittle or ductile mode through qualitative analyses [8]. Further, these data cannot be used to calculate specimen strain or related properties such as elastic modulus. The statistical analyses were performed using SAS 9.1 statistical software [11].

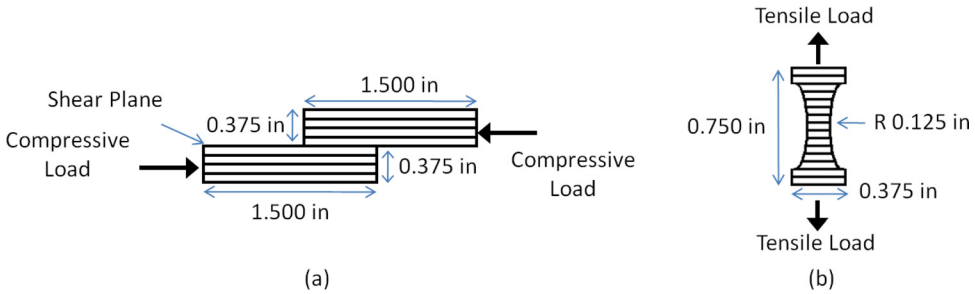

Fig. 1 Loading scheme and tape diagram of (*a*) shear and (*b*) tensile specimens—not to scale

2.2 Shear Testing. UAM shear specimens were built based on ASTM Standard Test Method for Lap Shear Strength of Sealants (ASTM C 961-06) [12]. The specimens were designed such that a tape layer was along the shear plane as shown by Fig. 1. The samples were tested in a shear jig where one leg is supported and the other leg is loaded from the top. Loading was applied at 0.127 mm/s until sample failure; measurements included force and hydraulic ram displacement.

2.3 Transverse Tensile Testing. UAM transverse tensile specimens were built such that the tape layers were perpendicular to the applied axial loading (Fig. 1). Since this geometry and test method was not based upon any known standard configuration, control tests were run with a solid wrought piece of 3003 aluminum. These tests show this geometry does not bias the ultimate tensile strength and is repeatable. The samples were axially loaded at 0.127 mm/s until failure while the force and hydraulic ram displacement were recorded.

2.4 Micrograph Preparation. After mechanical testing, the bond interface of selected samples was examined to determine a correlation between macroscopic mechanical strength and microstructure in UAM 3003 aluminum composites. Samples were cross-sectioned (perpendicular to weld direction) and hot mounted in a clear polymer matrix. Samples were then ground and polished using standard methods and observations were conducted on as-polished samples using an inverted (metallurgical) optical microscope under various magnifications.

2.5 UAM Bond Characterization. Optical micrographs of UAM cross sections were analyzed using ImageJ [13] image analysis software to assist in calculating the LWD. Multiple studies have examined the LWD of UAM built samples to quantitatively characterize the amount of bonding present at the interfaces [4,5,7]. LWD is defined as

$$\text{LWD} = \frac{\text{Bonded interface length}}{\text{Total interface length}} \times 100(\%) \tag{2}$$

Microstructural observations were conducted using an optical light microscope at 25× and 100× magnifications, the latter being used for LWD calculations. A five by five grid of micrographs was taken across the entire cross sectional face of each tested sample. Linear weld density was measured per micrograph with each micrograph showing about five interfaces (six tape layers) or a 1111 μm by 833 μm area. In total, 125 to 130 LWD measurements were taken and averaged to find the LWD per sample.

In ImageJ, a grayscale image threshold value was set at a constant value to delineate the void areas in all of the images. A resulting ratio of the total length minus the total void length over the total length per line was calculated. This procedure was repeated for all pictures of a given sample and the average of the measured LWD values was given as the total LWD for that given sample according to Eq. (2).

In addition to calculating the LWD, the amount of bonding was characterized by examining optical micrographs of UAM fracture surfaces. Fracture surface micrographs were taken of various shear and transverse tensile fracture surfaces at 25× and 52× magnifications, respectively. Only the top foil layer of the interfaces was used. This is because the surface of the bottom foil layer was textured by the horn during production while the top foil layer was only textured where contact and possible bonding occurred with the bottom layer. Five images were taken per shear fracture surface and three per transverse tensile fracture surface. A common nominal threshold was applied to all images and results were used to determine the percentage of bonded area with respect to total sample fracture surface area. The reported percent bonded area for a given sample is the percentage bonded area per image averaged across the total number of images for that sample.

Further study into the bonding characteristics was performed using scanning electron microscopy (SEM) to determine the metallurgical bonding between foils. Images were taken of fractured samples to calculate an area fraction of bonding using the amount of ductile failure present. SEM is necessary because the spatial resolution of SEM is much higher than optical microscopy, allowing for the investigation of ductile failure between foils [14]. For this study, the surfaces of two samples fractured in UTTS were investigated. Using SEM, 50 randomly located images on each of the two samples were taken on the surfaces of the top foil layer of the fractured samples where no direct horn contact took place. Secondary electron detection images at 2000× were used. A grid of 340 equally spaced points was overlaid on each image and each point was analyzed individually using the manual point count method. The features of interest analyzed in this study are described in Sec. 5.2. Due to the variability of the testing, each point was tested and analyzed twice independently.

3 Mechanical Test Results

Four treatment combinations did not produce samples that could be tested due to delamination during the building process. This is caused by a combination of reaching the critical height to width ratio (~0.7-1:1) that has been found to exist for parts built by UAM [15], and a lack of overall power (due to low oscillation amplitude) necessary to create sufficiently clean faying surfaces. All four treatment combinations that were not built had an oscillation amplitude of 18 μm with varying levels of tack force, weld force, and weld rate. Other samples are missing due to breakage during postprocess machining. Overall, 14 of the 18 treatment combinations could be built with at least one sample per combination for both shear and transverse tensile samples.

The breaking force varied considerably between samples within individual experiments and between experiments. Figure 2 shows the USS and UTTS averages over the sample replicates and the standard deviation, where the standard deviation represents the variability between samples or replicates. The number of samples tested for each experiment number is included above the bar for each combination. The recorded breaking force was the force at which the specimen underwent complete failure (significant

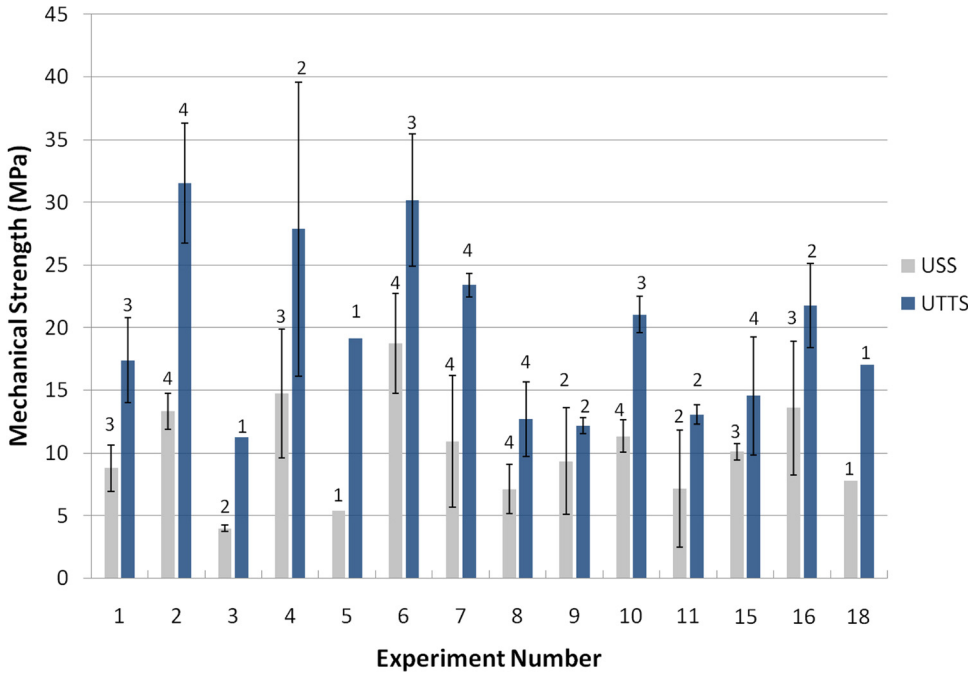

Fig. 2 Interval plot showing USS and UTTS experimental results–bars represent one standard deviation and numbers above each plot represent number of samples tested

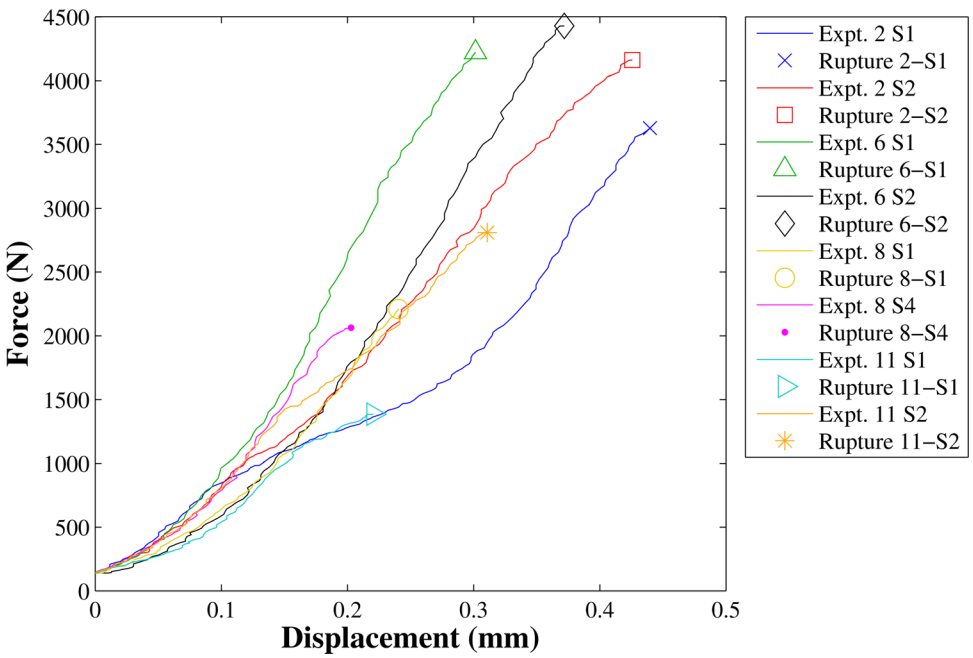

Fig. 3 Measured force versus displacement curves for shear tests

decrease in force). Failure occurred near the top of the gauge region in each of the samples. Figures 3 and 4 show force versus displacement curves for several low and high strength shear and transverse tensile samples, respectively. Both shear and transverse tensile tests resulted in a linear force–displacement relationship, indicating that samples failed in a macroscale brittle fracture mode caused by voids and inadequate bonding. However, the fracture area to be discussed later did indicate microscale ductile fracture similar to previous observations [8,16]. The higher strength samples had greater displacement than the low strength samples implying that there were a greater number of localized microscale areas that underwent ductile failure.

4 Statistical Analysis of Mechanical Strength Tests

4.1 Results of Analysis of Variance. The association between USS and UTTS data and four manufacturing parameters was analyzed statistically by fitting a linear model. The partition of the total variability in the response variables (USS and UTTS) due to different sources (model effects and random error) is typically shown in the analysis of variance (ANOVA) table. The adjusted type I error probability, α, selected for this experiment was 0.05 to test each of the model parameters, giving an overall error rate of at most 0.20 per mechanical test. The α level is the threshold probability of a false positive (type I error), that is,

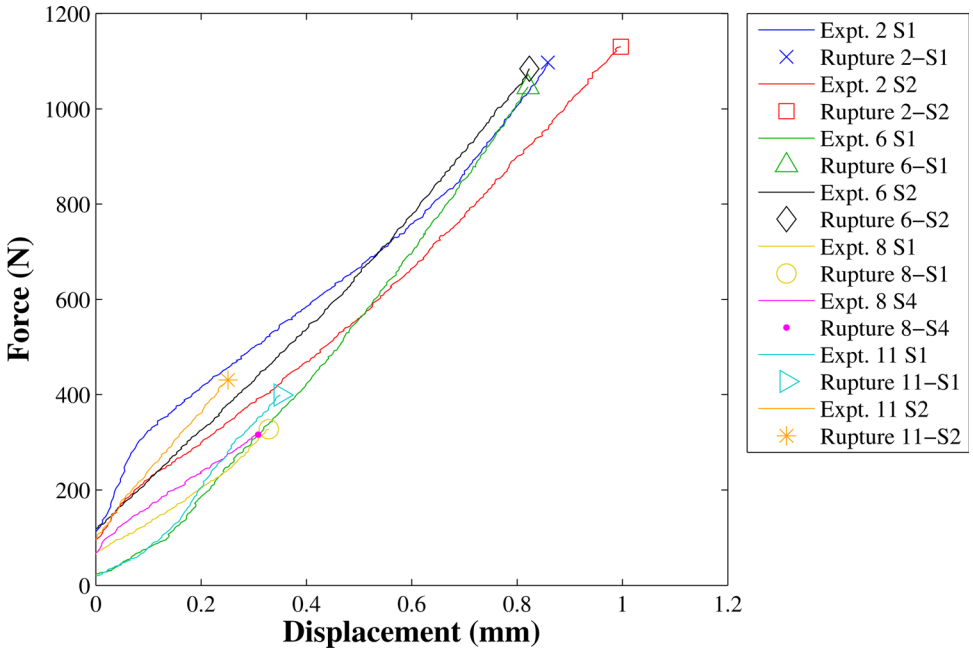

Fig. 4 Measured force versus displacement curves for transverse tensile tests

Table 5 ANOVA table for USS data

Source of variation	Degrees of freedom	Type III sum of squares	Mean square	F-ratio	p-value
Tack force	1	2.92	2.92	0.38	0.5506
Weld force	2	163.34	81.67	10.52	0.0019
Amplitude	2	33.16	16.58	2.14	0.1578
Weld rate	2	17.46	8.73	1.12	0.3546
Tack force, Weld force interaction	2	69.52	34.76	4.48	0.0332
Model total	9	336.91	37.43	4.82	0.0055
Error	13	100.97	7.77	—	—
Total	22	437.87	—	—	—

Table 6 ANOVA table for UTTS data

Source of variation	Degrees of freedom	Type III sum of squares	Mean square	F-ratio	p-value
Tack force	1	38.36	38.36	1.98	0.1826
Weld force	2	311.91	155.95	8.06	0.0053
Amplitude	2	211.85	105.92	5.47	0.0189
Weld rate	2	100.07	50.04	2.59	0.1134
Tack force, Amplitude interaction	2	82.16	41.08	2.12	0.1593
Model total	9	911.10	101.23	5.23	0.0039
Error	13	251.60	19.36	—	—
Total	22	1162.70	—	—	—

rejecting the null hypothesis when it is true. The p value represents the probability of obtaining a test at least as extreme as the one observed, assuming that the null hypothesis of no trend or no effect is true. The lower the p value the stronger the evidence against the null hypothesis; when $p < \alpha$, the null hypothesis is rejected in favor of the alternative hypothesis (there is a trend or an effect).

The experimental runs that could not be tested were removed from the DOE. Padding the response matrices with zeros or other forms of data manipulation is not possible in this case as not enough is known about the USS and UTTS for these composites. The ANOVA was then performed on the remaining USS and UTTS data based on the model given by Eq. (1) with the corresponding interaction term added. The ANOVA tables are shown in Tables 5 and 6.

The results from the ANOVA for the USS data (Table 5) show that the p values for tack force and weld rate are greater than $\alpha = 0.05$, so the null hypotheses cannot be rejected for these effects. Therefore, different levels of tack force and weld rate used in this DOE do not have a significant effect on the USS of UAM built samples. Weld force has $p < \alpha$, thus the null hypothesis can be rejected in favor of the alternative. It is concluded that there is a significant effect of different levels of weld force on the response variable USS.

Table 5 shows that amplitude is not significant with $p > \alpha$, but this p value does not reflect that four of the six treatment combinations with amplitude at its lowest level (18 μm) could not be tested. When considering that these treatment combinations with the lowest amplitude did not produce viable samples (and hence, no USS data), it is apparent that amplitude does play a role in the USS of UAM builds even though the ANOVA calculations do not reflect this fact. We conclude that there is a critical amplitude for bonding to occur above which amplitude does not have a significant effect on USS (according to the ANOVA).

It was found that there is an interaction between tack force and weld force ($p < \alpha$). In order to further investigate this effect, an interaction plot was created to visualize the relationship between these two effects, as discussed in Sec. 4.2.

Table 6 illustrates that tack force and weld rate for UTTS data both have $p > \alpha$. Therefore, it is concluded that there is not a significant effect of different levels of these factors on the response variable UTTS. Weld force has $p < \alpha$ from the ANOVA table and therefore has a significant effect on UTTS. The effect of amplitude yielded $p < \alpha$, suggesting that amplitude does significantly affect the UTTS even though there are certain treatment combinations with low amplitude that could not be built.

The interaction between tack force and amplitude was included in the model for UTTS data and although the p value is greater than 0.05, this term reduced the overall model error and was kept in the model.

4.2 Interaction Plots. Pairwise interaction terms were included in the model. Given the limited degrees of freedom due to relative small sample sizes, one interaction term at a time was studied. Each of the interactions between parameters was studied in relation to the UTTS and USS, however, only the interaction of tack force and weld force for USS was found to be significant with $p < \alpha$

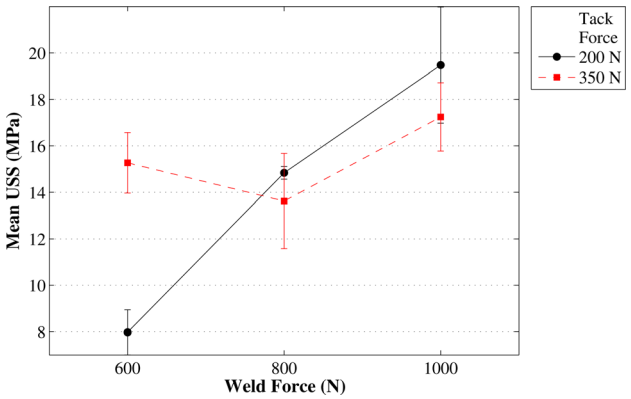

Fig. 5 Interaction plot between tack force and weld force for USS data

from the ANOVA. All other interactions had $p > \alpha$ and were therefore determined to be insignificant. Table 6 shows one example of an insignificant interaction with tack force and amplitude.

The interaction plot for tack force and weld force in relation to USS is shown in Fig. 5. For a 600 N weld force, a 350 N tack force produces a higher USS. Then, at 800 N weld force, a slightly higher USS is produced with a 200 N tack force. This is again shown at 1000 N weld force with a tack force of 200 N producing a higher USS. Due to this situation, standard error bars were added to the interaction plot. The error bars overlap for levels of tack force at the 800 N and 1000 N levels of weld force, but not at the 600 N level. Therefore, it is very likely that a significant difference between the levels of tack force at the 600 N level of weld force exists, but there is very little, if any, difference between levels of tack force at 800 N and 1000 N weld force. All other interactions with USS as the response variable were checked in this manner, and none was significant.

Table 7 P-values for trend contrasts in USS and UTTS data as a function of UAM process parameters

Mechanical response	Parameter	Straight-line trend p-value	Quadratic trend p-value
USS	Weld force	0.0005	0.6003
UTTS	—	0.0015	0.7679
USS	Amplitude	0.1671	0.7542
UTTS	—	0.0832	0.321
USS	Weld rate	0.1773	0.6445
UTTS	—	0.1405	0.0883

4.3 Scatter Plots and Trend Contrasts. Scatter plots of the average USS and UTTS data for each factor were created to detect trends. Figure 6 shows the averaged trends for each parameter for USS and UTTS data and shows simple model-fits (black lines) for the data. Based on these observations, straight-line and quadratic statistical trend contrasts for weld force, amplitude, and weld rate were examined.

Table 7 shows the results from the trend contrasts. Using a significance level of $\alpha = 0.01$ it is found that there is a straight-line trend present in the data for weld force (both USS and UTTS). There are no other significant trends reflected by the p values for any of the other parameters. It is noted though that because of the few number of samples for amplitude at 18 μm, the trend contrasts are most likely incorrect for this parameter. Consequently, it is more accurate to interpret the trends shown on the scatter plot for amplitude, in which there is a positive linear trend for both the USS and UTTS data.

Figure 6 shows that for both the USS and UTTS, the two significant parameters (weld force and amplitude) have a positive linear trend and produce their highest response at the highest level of each parameter. Therefore, for the levels of each parameter given in this DOE and based on the statistical analyses, a 3003

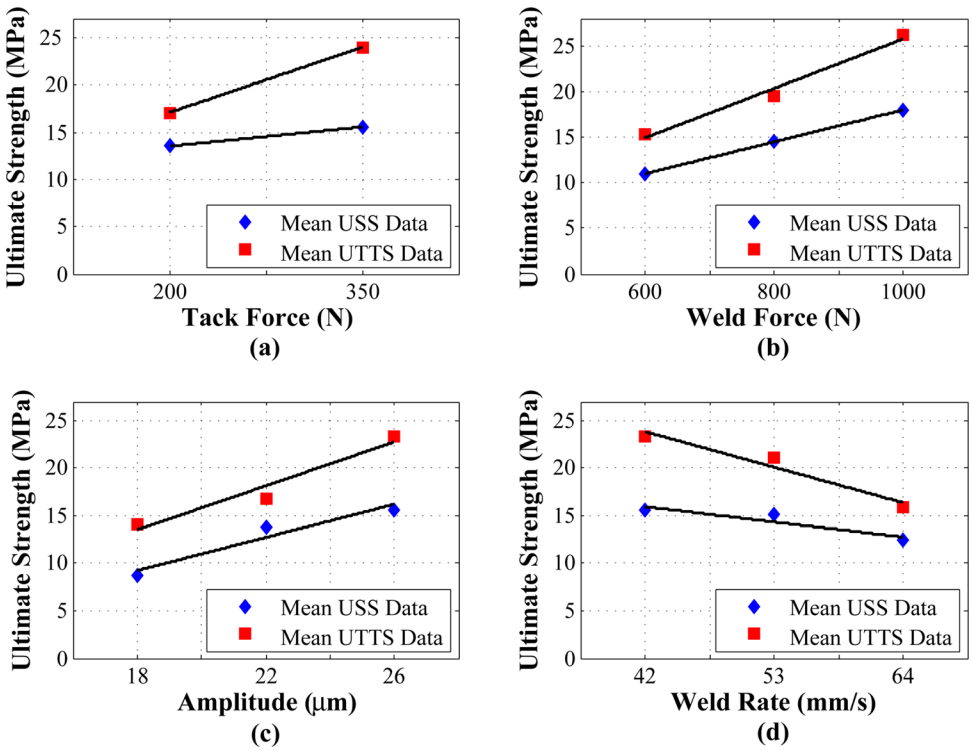

Fig. 6 Deviation in average USS and UTTS as a function of selected levels for each parameter: (*a*) Ultimate strength versus tack force, (*b*) ultimate strength versus weld force, (*c*) ultimate strength versus amplitude, and (*d*) ultimate strength versus weld rate

Table 8 Summary of experiments from which samples were viewed microscopically

Experiment number	Tack force (N)	Weld force (N)	Amplitude (μm)	Weld rate (mm/s)	USS (MPa)	UTTS (MPa)
1	350	600	22	42	13.3	17.4
2	350	1000	26	53	16.5	31.5
3	200	600	18	42	5.2	11.2
6	200	1000	26	42	20.0	30.2
8	200	600	26	64	8.1	12.7
10	200	800	26	64	14.6	21.0

aluminum specimen with maximized USS and UTTS would be built under the following parameters:

- Tack Force: 350 N
- Weld Force: 1000 N
- Amplitude: 26 μm
- Weld Rate: 100 or 125 IPM (42 or 53 mm/s)

5 Results of Microstructural Analysis

5.1 Optical Microscopy. LWD was examined for samples with high, medium, and low USS and UTTS, and LWD was calculated using Eq. (2). Table 8 summarizes the process parameter combinations for each experiment examined and the corresponding average mechanical strength. Typical images used for calculating LWD are shown in Figs. 7(*a*) and 7(*b*).

It can be seen that there are three distinct features at the interface. There are areas where large voids exist, areas where there are small cracklike voids and partial bonding, and areas where there is no visible interface in which it is assumed that there is full metallurgical bonding present. From Fig. 7(*b*), note that there are fewer large voids compared with the sample from Experiment 6 (Fig. 7(*a*)), but there are still visible interfaces with smaller, line shaped voids and defects. Figure 8 shows the full results of the LWD analysis performed for this DOE.

From Fig. 8 it can be seen there is no trend between mechanical strength of UTTS or USS and linear weld density. These results motivate that other, more objective methods be employed to investigate the relationship between mechanical strength of UAM builds and bond quality.

Fracture surfaces were therefore examined for both USS and UTTS samples similar to previous studies [17,18]. A sample micrograph before and after applying the image analysis threshold can be seen in Figs. 9(*a*) and 9(*b*), respectively. The dark, textured regions (marked as I in Fig. 9(*a*)) are assumed to be bonded areas, whereas the light, smoother regions (marked as II in Fig. 9(*a*)) are unaffected material.

Using ImageJ on images with a fixed threshold, the percentage of the detected bonded areas (black) to the overall area could be calculated. The results are displayed in Fig. 10. Both plots show

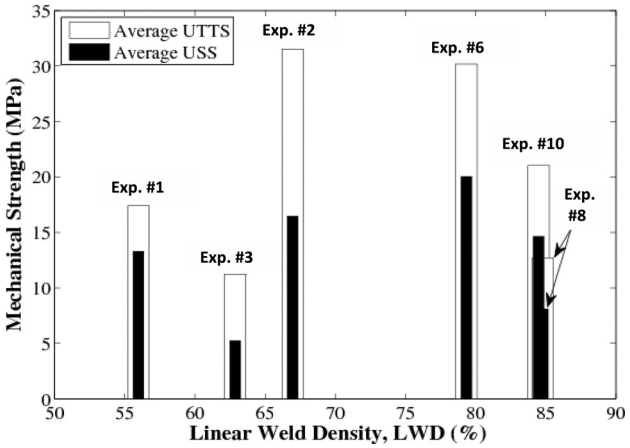

Fig. 8 LWD versus average mechanical strength (USS and UTTS) of UAM built Al 3003 specimens

that all of the samples have a relatively similar percent bonded area; between 35% and 45% for UTTS and between 30% and 50% for the USS samples. The range is slightly larger for the USS samples because of smearing of the bonded regions that can occur during testing, which increases the perceived ratio of dark areas to light areas seen in the images.

As the percentage of bonded area increases, the USS tends to increase but the UTTS shows no trend. It is unclear why one would increase while the other would show no relationship with bonded area. It is known that potentially bonded areas will be regions of greater height and deformation than unbonded regions because they would be in contact with the adjacent faying surface. However, it is difficult to conclude from the optical images that all of the dark, damaged areas were metallurgically bonded because they could also be areas that were in contact with the layer below, but not fully bonded. Therefore, SEM was employed to better understand why there is a significant difference in strength, but not in percent bonded area, especially in UTTS measurements.

5.2 Electron Microscopy. Fracture surfaces of samples from Experiments 2 and 8 previously broken during ultimate tensile testing were examined using a manual point count. The analysis consisted of defining each point on an overlaid grid as original machined surface, ductile failure, shear ductile failure, flow, or brittle shear. Each feature is defined below and sample images are represented in Fig. 11.

(i) Machined surface: Smooth, unabraided surface of upper foil. Machine lines normally present with small, dark dots following machine direction. Indicated no contact between the foil layers.

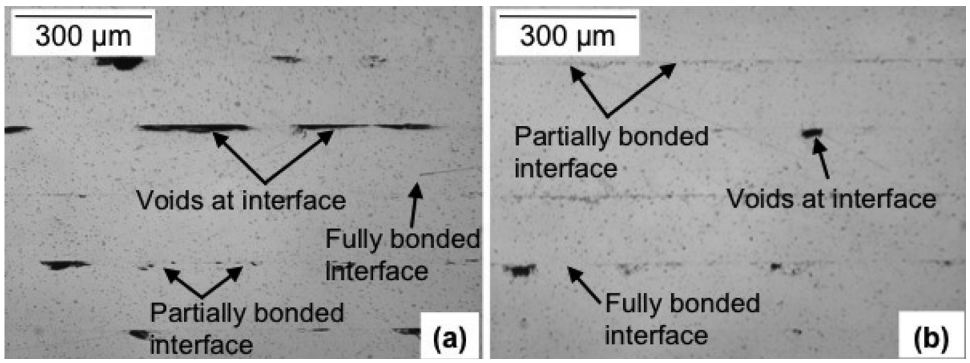

Fig. 7 Micrographs of (*a*) Experiment 6, Sample 2 (high USS and UTTS) and (*b*) Experiment 8, Sample 2 (low USS and UTTS) used in calculating total LWD

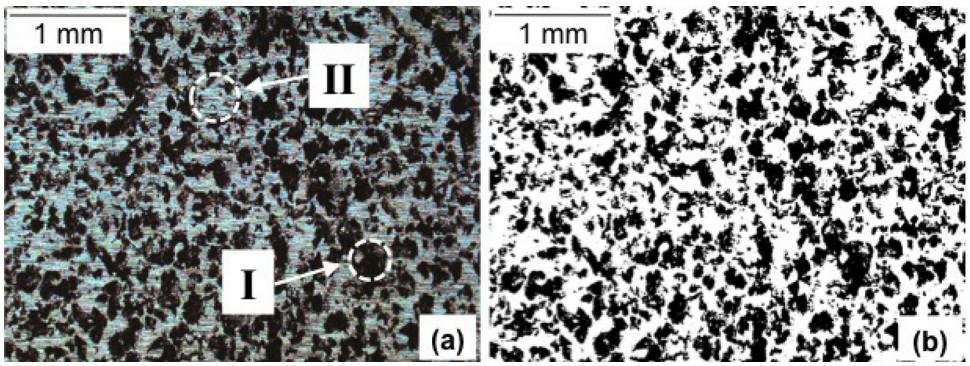

Fig. 9 Optical images of transverse tensile fracture surfaces (top surface) from Experiment #2 (*a*) before image processing and (*b*) after threshold adjustment. Region I is damaged material caused by bonding or contact with previous surface. Region II is material unaffected by the UAM process

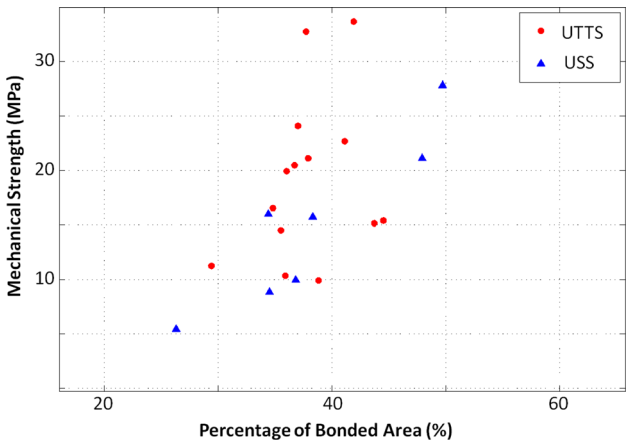

Fig. 10 Percentage of bonded area on fracture surfaces versus mechanical strength of both UTTS and USS samples

(ii) Ductile failure: Metallurgical bonding evidenced by the typical circular cup/cone type fracture.
(iii) Shear ductile failure: Determined to be ductile failure viewed at an angle not normal to the surface. Hypothesized to occur as the bonds are broken during tensile testing, foils tend to peel from one another producing ductile failure at a non-normal angle to the original foil surface.
(iv) Flow: Defined as texture produced due to foil to foil contact without creating a true metallurgical bond. In this case, peaks of material in the textured foil are hypothesized to press into the smooth upper foil creating an impression. The peaks displace material which flows out around the indentation as it is being pressed into.
(v) Brittle shear: Defined as a sheared off region without any ductility associated with its failure.

Areas measured as ductile and shear ductile failure were taken to represent metallurgical bonding as their failure mechanisms would be consistent with this type of bonding. Brittle shear and flow areas represent areas of foil to foil contact which could provide some strengthening through mechanical interlock. However, it is believed this type of bonding is much weaker than metallurgical bonding.

Due to the somewhat subjective nature of SEM fracture analysis, each point was tested and analyzed by independent investigators. The area fraction of each feature of interest was calculated and averaged between the two collected datasets. The averaged results are tabulated in Table 9.

Two results from the area fraction analysis are emphasized. The first is the area fraction of machined surface is about 7% higher for the lower strength sample (Experiment 8). The second is the area fraction of ductile regions in Experiment 2 is about 5% higher than in Experiment 8. The higher area fraction of ductile regions in Experiment 2 would tend to support the hypothesis that higher mechanical strengths are a result of a higher area fraction of metallurgical bonding. Conversely, UAM builds that exhibit

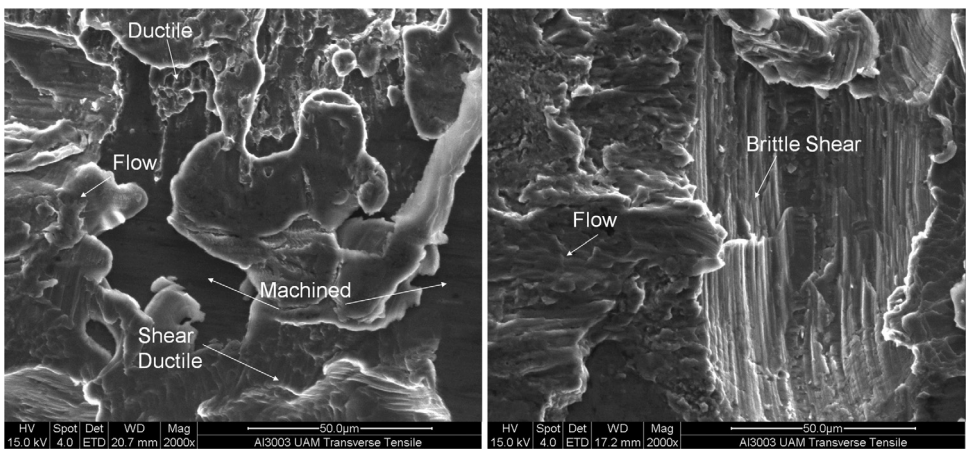

Fig. 11 Example SEM images representing shear ductile failure, ductile failure, flow, brittle shear, and machined surface

Table 9 Area fraction of features measured on fracture surface using SEM

Exp #	UTTS (MPa)	Machined (%)	Shear ductile (%)	Ductile (%)	Flow (%)	Brittle shear (%)	Combined ductile (%)
2	31.5	17.9	13.9	4.2	63.2	0.9	18.1
8	12.7	24.9	11.8	1.5	58.5	3.3	13.3

poor mechanical strengths are hypothesized to have a lower area fraction of metallurgical bonding. Using the area fraction of machined surface, it is hypothesized that a greater area fraction of contact between the foil layers could lead to more metallurgical bonds being formed, leading to higher strengths.

6 Discussion

From the results shown in Fig. 2, certain combinations had large standard deviations while others could not be built or only had one sample to test, yielding no standard deviation. These combinations could affect the significance of the data making them potentially insignificant when standard deviations are high or zero due to one or zero samples being tested. However, the models used were stable; with the model coefficients and significance consistent in the model building process. In addition, with the information calculated from the ANOVA, interaction plots, scatter plots, and trend contrasts, the resulting conclusions for the treatment combinations are deemed significant and meaningful for predicting mechanical strength for UAM builds. A larger sample size could provide more resolution by decreasing the standard error and providing more data points. However, these studies can be expensive and based on the information discovered in this work, may not provide significantly more meaningful information.

6.1 Mechanical Strength of Shear Specimens. Samples mainly displayed a predominantly linear force/displacement relationship, indicating a macroscale brittle failure. The highest standard deviation is 5.24 MPa for Experiment #7, which is 34% of the average USS for that experiment. Experiment #6 produced the highest strengths with an average of 20.03 MPa and a standard deviation of 4.01 MPa. This is still only about 18% of the USS of solid 3003 aluminum (110 MPa). Therefore, it can be implied that the total energy available for bonding in this DOE was not high enough to create builds with ultimate shear strengths comparable to solid 3003 aluminum.

6.2 Mechanical Strength of Transverse Tensile Specimens. All samples exhibited a predominantly linear force/displacement relationship. The samples all failed at a single weld interface and produced two separate pieces, both indicating a macroscale brittle failure. There is substantial deviation in UTTS with the highest standard deviation being 11.73 MPa (42% of average value for Experiment #4). Experiment #2 produced the highest strengths with an average of 31.52 MPa and a standard deviation of 4.78 MPa. This is only about 16% of the ultimate tensile strength of solid 3003 aluminum (200 MPa).

The discrepancy between the experiment with the highest mechanical strength (Experiment #6 for shear tests; Experiment #2 for tension tests) can be explained by examining the combination of process parameters for each experiment. Both experiments had a weld force of 1000 N and amplitude of 26 μm, but the tack forces and weld rates were different. This result agrees with the conclusions of the statistical analysis that normal force and amplitude are significant parameters, but tack force and weld rate are not. The percent difference between the USS of Experiment #2 and Experiment #6 is only 19%. The percent difference between the UTTS of Experiment #2 and Experiment #6 is only 4%. Therefore, production of a high strength sample requires the highest level of weld force and amplitude in this DOE, while weld rate and tack force could be at any of their levels in this study.

6.3 Effects of Manufacturing Parameters. The results of the ANOVA including the interaction plots and statistical trend analyses lead to the conclusion that weld force and amplitude have a significant effect on the USS and UTTS of UAM built samples. The physical explanation for the effects of these two parameters is discussed below in detail. While tack force and weld rate were not found to have a significant effect on the outcome measures (USS and UTTS) they too are examined.

6.3.1 Effect of Tack Force. From the statistical analyses, tack force was not found to affect the USS or the UTTS. The tack force is needed for the operation of the machine, but the force needed for this step does not change the overall strength of the build because the levels used are too low to induce bonding. The tack force is just enough to imprint the horn texture onto the metallic tape and create a roughness. The added roughness increases the friction between the tape layers, and thus prevents the tape from becoming misaligned during the subsequent weld pass.

6.3.2 Effect of Weld Force. The USS and UTTS, increases as the level of weld force increases as shown in Fig. 6(*b*). Solid state bonds are formed due to metallic bonding when oxide and contaminant free metal surfaces are brought into intimate contact [19]. Metallic bonding occurs because valence electrons in metals are not bound to any particular atom [20]. Therefore, they are able to drift throughout the metal resulting in atomic nuclei with ionic cores. These drifting electrons bind the ion cores together in a lattice structure [20]. Therefore, metallic bonds can be created between two metal pieces by establishing intimate contact between oxide and contaminant free areas without the formation of a liquid phase. In order to achieve the necessary closeness of the metal atoms, a high normal force is required. As normal force is increased, surface asperities are crushed and the faying surfaces are brought into close contact so that the valence electrons can jump between the atoms of one faying surface to the atoms of the other creating the metallic bond [21]. Further, an increase in applied normal force increases the magnitude of the resultant interfacial shear stresses which aids in bond formation [7]. Therefore, for a maximized USS and UTTS of 3003 aluminum specimens built using the test equipment shown in these studies, a weld force of 1000 N should be employed.

6.3.3 Effect of Oscillation Amplitude. Like weld force, oscillation amplitude was found to have a positive linear effect on the USS and UTTS (Fig. 6(*c*)). The higher the oscillation amplitude, the higher the amount of applied ultrasonic energy. This energy combined with the normal force (weld force) determines the total energy available for bond formation during the welding process [7]. The amplitude aids in the destruction of the oxide layer and contaminant film which allows for clean metal-to-metal contact between the mating surfaces [19]. Furthermore, an increase in amplitude increases the magnitude of the shear forces and the resulting amount of local plastic deformation of surface asperities. Both of these factors are favorable for the formation of intimate nascent metal and subsequent strong metallic bonds. Further studies are necessary to fully assess the effect of oscillation amplitude, but the present research shows that an amplitude of 26 μm produces the best results.

6.3.4 Effect of Weld Rate. While not being statistically significant, weld rate still has an effect on the USS and UTTS of the specimens. Weld rate was found to have a relatively negative linear effect on the USS and UTTS over the parameter range, as can be seen in Fig. 6(*d*). The USS and UTTS decreased with an increase in weld rate. Weld rate determines the amount of energy per unit length or, alternatively, the amount of time over which energy is applied to a given point during the welding process [7]. Increasing the weld rate decreases the amount of time that the ultrasonic energy input can occur, resulting in insufficient interfacial

stresses causing inadequate oxide layer removal and nascent surface formation. Hence, the overall strength of the specimen decreases as well. For this DOE, there was not a great enough difference between the levels of weld rate in order for there to be a significant decrease in strength between levels. It is presumed that over a larger range of weld rates, a substantial difference in mechanical strength would be observed. Therefore, in order to decrease manufacturing time yet retain a relatively high level of mechanical strength, it is recommended that a weld rate of 53 mm/s (125 in/min) be used based upon the results of this research.

6.4 UAM Microstructure Characterization. The studies involving optical measurements of linear weld density have shown a poor correlation between bond density and bond strength making this type of examination inappropriate for determining UAM build strength. Optical measurements of fracture surfaces likewise were ineffective at comparing bond density and bond strength, especially UTTS. Due to resolution limitations, these types of measurements are only able to determine the fraction of contact area between foil layers, not the fraction of actual bonding. These results made it necessary to conduct manual point count SEM analysis on fracture surfaces to measure the area fraction of metallographic bonding. This analysis proved effective at correlating the UAM build strength to the fraction of ductile failure. The SEM work showed that there was approximately 5% higher ductile failure in the higher strength sample (Experiment #2) than the lower strength sample (Experiment #8). Furthermore, Experiment #2 had a LWD of 67%, while Experiment #8 had a LWD of 85%, a result contrary to intuition where higher bond density would correlate to ultimate tensile strength measurements. This method also showed that there was 7% more original machined surface present in the low strength sample, leading to the conclusion that there is less foil to foil contact in the low strength sample.

These results provide the basis for discontinuing the use of LWD measurements as a method of determining UAM build strength. Linear weld density can only measure the fraction of voids present in a material cross section without specific information about metallurgical bonding between foil layers, therefore it cannot be related to mechanical strength. The scanning electron microscopy point count measurements of UAM build fracture surfaces is much more versatile as it is able to determine fractions of bonding and surface contact between foil layers. Further applications of this method will be necessary to verify the statistical significance of the relationship between metallurgical bond area fraction and mechanical strength.

From the SEM analysis, it is shown that along a weld interface there is discontinuous bonding. Each area of bonding plastically deforms during loading, however, each area may show different strain hardening behavior during deformation. The varying strain hardening behavior makes it impossible to use the area of ductile failure alone to rationalize the mechanical strengths measured during testing. In addition, mechanical interlock between foil layers pressed into one another could provide a strengthening mechanism. In this case, texture on the foil surface would fit together without creating a metallurgical bond. This mechanism would provide some strengthening but far less than metallurgical bonding between layers. Due to the difficulties associated with measuring this mechanism, quantifying mechanical interlock was not pursued.

In the future, applications of the SEM point count method could be used on subsequent builds to provide further verification of its accuracy as well as provide insight into the parameter sets that produce the highest strengths. In addition, it may be worthwhile to investigate automated methods of measuring the regions of interest such as the using Fourier transforms or fractal analysis to conserve time.

7 Conclusions

A design of experiment utilizing a Taguchi mixed array was performed on 3003 aluminum composites for four process parameters—one at two levels (tack force), and the other three at three levels each. Pilot experiments elucidated the combinations of parameter levels that produce usable UAM builds. Shear and transverse tensile samples were created and tested; samples failed mainly in a macrobrittle fracture mode. An analysis of variance, interaction plots and trend contrasts were utilized for examining the USS and UTTS data.

The results of these analyses show that the parameters weld force and oscillation amplitude have a statistically significant influence on the resulting mechanical strength (USS and UTTS) of the specimens. Thus, it is put-forth that the following combination of levels of process parameters examined in this DOE produce the highest strengths: tack force of 350 N, weld force of 1000 N, oscillation amplitude of 26 μm, and weld rate between 42 mm/s (100 in/min) and 53 mm/s (125 in/min). Interface microstructure analyses including LWD and percent bond area characterizations were unable to correlate the bond area to mechanical strength. However, studies involving SEM of fracture surfaces showed a relationship between bond area and strength. These studies showed that a higher area fraction of metallic bonding in a sample related to a higher ultimate transverse tensile strength.

References

[1] Graff, K., 2005, *New Developments in Advanced Welding*, Woodhead Publishing Limited, Cambridge, England, pp. 241–269
[2] White, D., 2003, "Ultrasonic Consolidation of Aluminum Tooling," Adv. Mater. Processes, **161**(1), pp. 64–65.
[3] Hopkins, C., Fernandez, S., and Dapino, M., 2010, "Statistical Characterization of Ultrasonic Additive Manufacturing Ti/Al Composites," J. Eng. Mater. Technol., **132**, p. 0410061.
[4] Kong, C., Soar, R., and Dickens, P., 2004, "Optimum Process Parameters for Ultrasonic Consolidation of 3003 Aluminum," J. Mater. Process. Technol., **146**(2), pp. 181–187.
[5] Kulakov, M., and Rack, H., 2009, "Control of 3003-H18 Aluminum Ultrasonic Consolidation," J. Eng. Mater. Technol., **131**, p. 021006.
[6] Kong, C., Soar, R., and Dickens, P., 2003, "Characterisation of Aluminum Alloy 6061 for the Ultrasonic Consolidation Process," Mater. Sci. Eng., A, **363**(1–2), pp. 99–106.
[7] Janaki Ram, G., Yang, Y., and Stucker, B., 2006, "Effect of Process Parameters on Bond Formation During Ultrasonic Consolidation of Aluminum Alloy 3003," J. Manuf. Syst., **25**(3), pp. 221–238.
[8] Schick, D., Hahnlen, R., Dehoff, R., Collins, P., Babu, S., Dapino, M., and Lippold, J., 2010, "Microstructural Characterization of Bonding Interfaces in Aluminum 3003 Blocks Fabricated by Ultrasonic Additive Manufacturing," Weld. J., **89**, pp. 105s–115s.
[9] Montgomery, D., 1991, *Design and Analysis of Experiments*, John Wiley & Sons, New York.
[10] Dean, A., and Voss, D., 1999, *Design and Analysis of Experiments*, Springer, New York.
[11] Inc., S. I., 2002–2003, "Sas 9.1 copyright (c)".
[12] International, A., 2006, "C 961-06: Standard Test Method for Lap Shear Strength of Sealants."
[13] Abramoff, M., Magelhaes, P., and Ram, S., 2004, "Image Processing With Image J," Biophotonics Int., **11**(7), pp. 36–42.
[14] Lloyd, G. E., 1987, "Atomic Number and Crystallographic Contrast Images With the SEM: A Review of Backscattered Electron Techniques," Miner. Mag., **51**, pp. 3–19.
[15] Robinson, C., Zhang, C., Janaki-Ram, G., Siggard, E., Stucker, B., and Li, L., 2006, "Maximum Height to Width Ratio of Free-Standing Structures Built by Ultrasonic Consolidation," *Proceedings of the 17th Solid Freeform Fabrication Symposium*, Austin, TX.
[16] Dehoff, R., and Babu, S., 2010, "Characterization of Interfacial Microstructures in 3003 Aluminum Alloy Blocks Fabricated by Ultrasonic Additive Manufacturing," Acta Mater., **58**, pp. 1–12.
[17] Hahnlen, R., 2009, "Development and Characterization of NiTi Joining Methods and Metal Matrix Composite Transducers With Embedded NiTi by Ultrasonic Consolidation," Master's thesis, The Ohio State University, Columbus, OH.
[18] Zhang, C., Deceuster, A., and Li, L., 2009, "A Method for Bond Strength Evaluation for Laminated Structures With Application to Ultrasonic Consolidation," J. Mater. Eng. Perform., **18**(8), pp. 1124–1132.
[19] Mohamed, H., and Washburn, J., 1975, "Mechanism of Solid State Pressure Welding," Welding J., **55**, pp. 302s–310s.
[20] Kittel, C., 1995, *Introduction to Solid State Physics*, 7th ed., John Wiley & Sons, Canada.
[21] Parks, J., 1953, "Recrystallization Welding," Welding J., **32**(5), pp. 209s–222s.